

# DYNAMIC ANALYSIS OF THE EFFECT OF CENTRIFUGAL AND CORIOLIS FORCES IN SWINGING A BAT

Yoshiyuki Mochizuki, Tomoyuki **Matsuo**<sup>1</sup>, Suiji **Inokuchi**<sup>1</sup>, and Koichi **Omura**<sup>2</sup>

\*Laboratories of Image Information Science and Technology, Osaka, Japan

<sup>1</sup>Osaka University, Osaka, Japan

<sup>2</sup>Takarazuka University of Art and Design, Hyogo, Japan

This paper reports a dynamic analysis by computer simulation of bat swinging, taking into account inertial forces at the wrist joint, and which consist of centrifugal and Coriolis forces generated from a body turn and internal rotation of the upper limbs. The ideal bat swing generated by optimisation using a mathematical model is also described. Based on the dynamic analysis, it is shown that the inertial forces play an important role in the process of flexion and extension between a bat and the upper limbs during a bat swing, and that the effects of gravity on a bat is much smaller than those from inertial forces. It was also proven from the optimisation that an ideal bat swing, a swing using minimal torque at the wrist, exists.

KEYWORDS: computer simulation, mathematical model, inertial force, optimisation

INTRODUCTION: When a person swings a bat, the process of flexion-extension-flexion at the wrist joint can be observed. Figure 1 illustrates this flexion-extension-flexion displayed by a professional baseball player. The first part of the flexion-extension process is usually assumed to be caused by the effect of a centrifugal force resulting from a body turn, and gravity acting on the bat. As the bat is also affected by internal rotation generated by the crossing motion of the upper limbs during a bat swing, another inertial force, Coriolis force (gyro effect), must act on the wrist joint. The purpose of the present study was to analyse the dynamic interaction between the bat and upper limbs, at the wrist joint, using computer simulation and a custom-designed simple mathematical model. The mathematical model has also been used to determine the ideal bat swing, using the consequences of the analysis, by an optimisation with a quasi-Newton method.

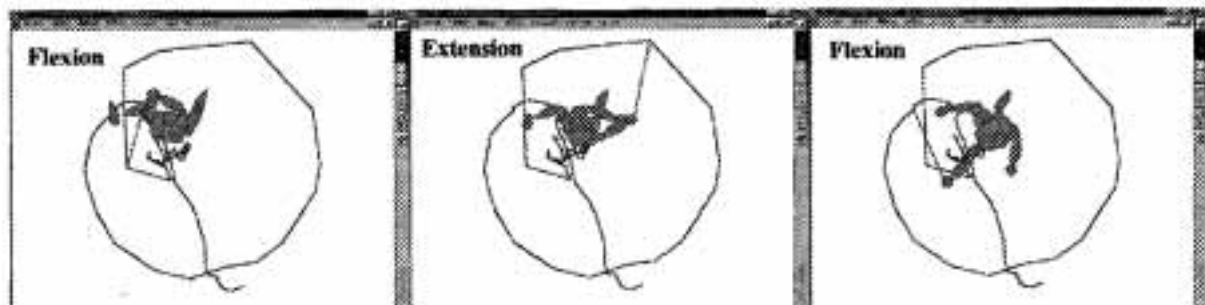


Figure 1 - **Process** of flexion-extension-flexion in a bat swing

METHODS: Figure 2 indicates our mathematical model for a bat swing that consists of three segments; a trunk, an upper limb, and a bat. There are three degrees of freedom in the model. We constructed a very simple mathematical model in order to make evident the dynamic interaction at the joint between a bat and an upper limb. The inertia tensor of each segment is calculated by numerical integration with an approximation by a curved surface. D-H representation (Denavit and Hartenberg, 1955) is applied to the local coordinate system defined at each joint, where the x-axis coincides with the longitudinal axis of the segment. When  $A_i$  is the 4x4 matrix that transforms the expression on the i-th local coordinate system to the expression on the i-1-th local coordinate system, and  $T_i = A_0 A_1 \dots A_i$ , the Lagrange equation for  $\tau_2$  at the joint between the bat and the upper limb can be represented by the following equation:

$$\tau_2 = \sum_{j=1}^n \text{tr} \left[ \frac{\partial T_1}{\partial \theta_2} \cdot j_1 \frac{\partial T_1}{\partial \theta_2} \right] \dot{\theta}_1 + \sum_{j=1}^n \text{tr} \left[ \frac{\partial^2 T_1}{\partial \theta_2 \partial \theta_2} \cdot j_1 \frac{\partial T_1}{\partial \theta_2} \right] \dot{\theta}_2 + \dots + \tau_{2F} \quad (1)$$

where  $r_i$  is the position vector of the centre of gravity for each segment, and  $g$  is the vector of the gravitational acceleration. Lagrange equations at other joints can be expressed in the same way. In equation (1), the first term is about the acceleration of each joint angle, the second term expresses the sum of centrifugal forces and Coriolis forces, and the last term represents the effect of gravity on the bat. Simulation experiments for dynamics analysis were executed as follows: 1. Fixing  $\theta_2$  to some values, 2. Providing the appropriate input data for  $\theta_0$  and  $\theta_1$ , 3. Calculating each torque by inverse dynamics from Lagrange equation, 4) Investigating the values of each term in the equation (1) at each time. The fixing values of  $\theta_2$  are Condition A: 0 (rad), B:  $-\pi/6$ , C:  $-\pi/3$ , D:  $-\pi/2$ , E:  $-2\pi/3$ , and F:  $-5\pi/6$ , the input data for  $\theta_0$  and  $\theta_1$  are determined by based on the following equation (2) and equation (3) that are same as the initial data for the optimising calculation indicated in Graph 5.

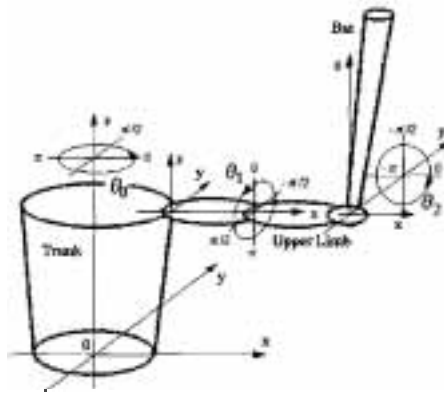


Figure 2 - Mathematical model

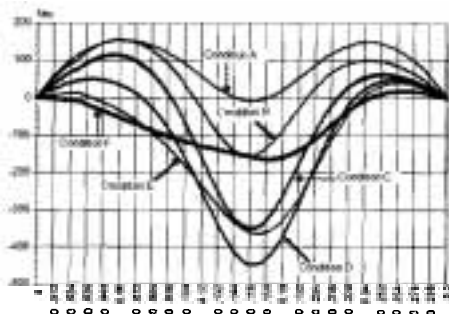
$$p(t) = \pi^3(6t^2 - 15t + 10) \quad (2) \quad q(t) = -\pi^3(6t^2 - 15t + 10) + \pi/2 \quad (3)$$

The physical data for the simulation are indicated in Table 1. The optimising calculation is executed to all three degrees of freedom by a quasi-Newton method that consists of the calculation of Hessian by the Broyden-Fletcher-Goldfarb-Shanno (BFGS) formula and the calculation of the search vector by secant method and Wolfe's condition (Fletcher, 1980) (Mochizuki et al., 1997a; 1997b; 1998). The initial time sequence data of  $\theta_2$  for the optimising calculation was appropriately generated from the consequences of the above simulation experiments and it is shown in Graph 5. The objective function comprises of the penalty of the movability for each joint, the penalty of the maximum torque for the wrist joint, the penalty of the maximum velocity of a bat head (50 m/s), the terms of the smooth acceleration and braking for a bat, the total torque described by  $L^2$  norm type expression, and the total torque derivatives of the first and the second degrees described by  $L^2$  norm type.

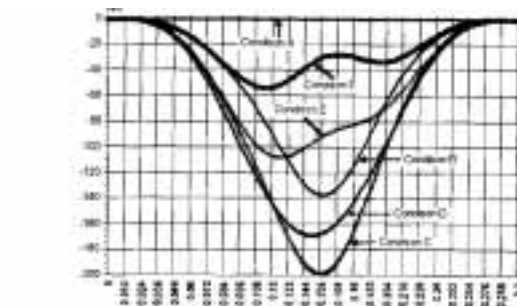
Table 1 Physical Data

	Mass (kg)	Inertia Tensor Hxx (m <sup>2</sup> kg)	Inertia Tensor Hyy (m <sup>2</sup> kg)	Inertia Tensor Hxz (m <sup>2</sup> kg)	Inertia Tensor Hxy (m <sup>2</sup> kg)	Inertia Tensor Hyy (m <sup>2</sup> kg)	Inertia Tensor Hxz (m <sup>2</sup> kg)
Body	32.257	1.9473	1.6952	$4.3052 \times 10^{-1}$	$-1.2785 \times 10^{-5}$	$-6.7668 \times 10^{-4}$	$2.2097 \times 10^{-4}$
Upper Limb	3.5184	$3.3700 \times 10^{-3}$	$1.2443 \times 10^{-1}$	$1.2490 \times 10^{-1}$	$3.6439 \times 10^{-4}$	$-9.2016 \times 10^{-6}$	$1.1308 \times 10^{-3}$
Bat	$8.68 \times 10^{-1}$	$2.8519 \times 10^{-4}$	$4.8076 \times 10^{-2}$	$4.8076 \times 10^{-2}$	$4.4247 \times 10^{-6}$	$1.292 \times 10^{-7}$	$4.4247 \times 10^{-6}$

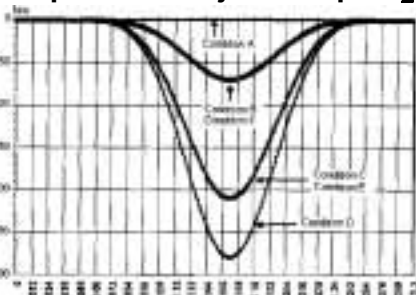
RESULTS AND DISCUSSION: Since the torque  $\tau_0$  for a body turn was affected by the state of the upper limb and the bat, it tended to be increased in conditions A, B, and C at the acceleration and the braking because their inertia tensors were larger than in conditions D, E, and F, roughly speaking. For the same reason, the torque  $\tau_1$  for internal rotation of the upper limb tends to be increased in conditions D, E, and F. However, in the case of the torque  $\tau_2$ , it was more complex as shown in Graph 1, and we should investigate it in more detail.  $\tau_2$  works for the extension torque if  $\tau_2 \geq 0$  and it works for the flexion torque if  $\tau_2 \leq 0$ . However, we should remark that the bat will move to the opposite direction of  $\tau_2$  since  $\theta_2$  is fixed.



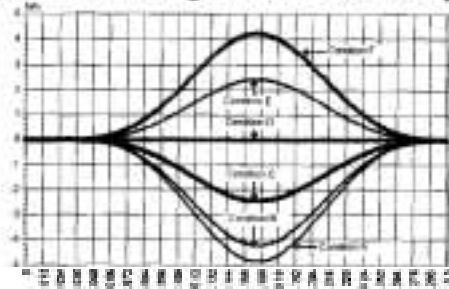
Graph 1 - Wrist joint torque  $\tau_2$



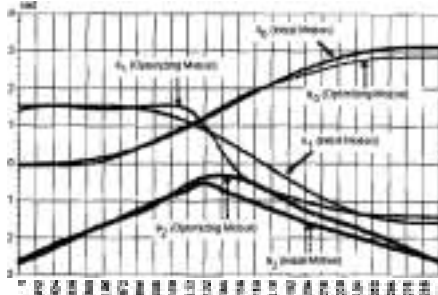
Graph 2 - Centrifugal force from body turn



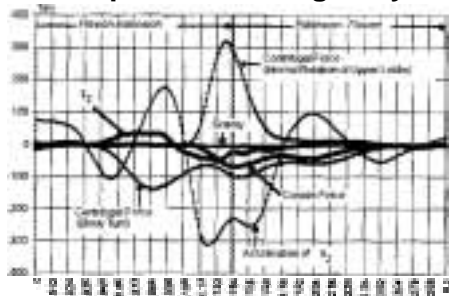
Graph 3 - Term of Coriolis force



Graph 4 - Term of gravity



Graph 5 - Initial and consequent joint angle



Graph 6 - Torque value of each term in optimising motion

In other words, the bat will move to the extension direction when  $\tau_2 \neq 0$ , and the bat will move to the flexion direction when  $\tau_2 < 0$ . The value of the term about the acceleration of  $\theta_2$  always works for the extension torque except the condition F, and it becomes smaller in turn the condition A, B, ..., and F. The value of the term about the acceleration of  $\theta_1$  is always 0 in the condition A and D. In cases B and C, the graph of them is same and it repeats  $\tau_2 \geq 0$ ,  $\tau_2 < 0$ ,  $\tau_2 \geq 0$ , and  $\tau_2 < 0$  with shaping the point symmetry (about  $t=1.65$  s, torque=0). In cases E and F, their shape of the graph is the axial symmetry to the graph in B and C with respect to the time axis. Graph 2 shows the centrifugal force from the body turn and Graph 3 indicates the Coriolis force from the body turn and the internal rotation. Since these forces are all negative, the bat will move to the extension direction due to the effect of these forces for the same reason explained above. When comparing these two graphs, it seems that the effect from the Coriolis force is larger than the centrifugal force. However, since it depends on the condition of the experiments, we can not conclude it. Graph 4 shows the gravity and the bat will move to the extension direction in cases A, B, and C. The bat will move to the flexion direction in cases E and F, and in the case D, it does not work. However, from Graph 4, we can conclude that the effect from gravity is much smaller than the effect from the centrifugal force and the Coriolis force. Graph 5 indicates joint angle of the initial motion and the resultant motion after the optimising calculation. From the graph, we can understand that the more rapid internal rotation occurs near the peak of  $\theta_2$  in the optimising motion than in the initial motion. Graph 6 shows the torque graph of  $\tau_2$  and each terms of the equation (1), and Graph 6 shows that the centrifugal force from the body turn only works at first in the process of flexion-extension. The Coriolis force additionally works following the rapid internal rotation of the upper limbs from the end of the process of flexion-extension, and at the same

time, the centrifugal force from internal rotation of the upper limbs acts to the flexion direction over the process of extension-flexion. We can also see that  $\tau_2$  was kept small by combining the opposite values obtained from each term though the value of each term is not small. With respect to the velocity of the bat head, we could see that internal rotation works to increase the velocity of the bat head in cases B and C, and additionally, the velocity in the optimising motion reached 50 m/s according to the penalty condition. Figure 3 indicates the consequent motion from the optimising calculation with the trajectory of the bat head, where the direction of the bat swing is clockwise.

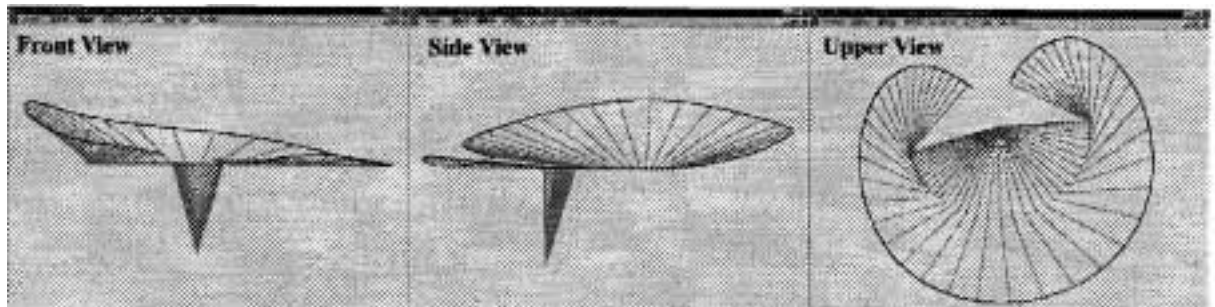


**Figure 3 - Optimising motion**

**CONCLUSION:** The inertial forces generated by the body turn and internal rotation of the upper limbs during a bat swing greatly influence the extension and the flexion which occurs between the bat and the upper limbs. In particular, the **Coriolis** force plays a very important role in executing the flexion-extension process of at the wrist joint, whereas the effect of gravity is much smaller than the effect from the inertial forces. As the **Coriolis** forces are larger than were anticipated, these forces may predispose a batter to wrist injury if they are not adequately controlled. To prevent such an injury it is recommended that a batter execute the body turn during batting smoothly while internally rotating both upper limbs effectively. This internal rotation will also be beneficial by increasing velocity of the bat head. The results of the optimising calculation presented in this study have also proven that there exists an ideal bat swing that can be achieved using minimal torque at the wrist joint. As the process of flexion-extension-flexion can be observed in other sports, such as the golf swing and the tennis serve, the findings of the present analysis of batting may be applied to these activities.

#### **REFERENCES:**

- Denavit, J. and Hartenberg, R. (1955). A kinematic notation for lower-pair mechanism based on matrices. *ASME Journal of Applied Mechanics*, 22, 215-221.
- Fletcher, R. (1980). *Practical Methods of Optimization*. John Wiley and Sons, Vol.1.
- Mochizuki, Y., Matsumoto, T., Tezuka, K., Yamashita, S., Inokuchi, S., Omura, K. (1997a). Computer Simulation of Generating Artificial Proficient Motion for Upper Limb during Baseball Pitching. *Proceedings 1997 International Symposium on Nonlinear Theory and its Applications Vol.1*, 401-404.
- Mochizuki, Y., Amano, H., Tezuka, K., Matsumoto, T., Yamashita, S., Omura, K. (1997b). Computer Simulation for Upper Limb during High Speed Baseball Pitching. *Theoretical and Applied Mechanics, Vol.46*, 271-277.
- Mochizuki, Y., Matsumoto, T., S., Inokuchi, S., Omura, K. (1998). Computer Simulation of the Effect of Ball Mass and Shape to Upper Limb in Baseball Pitching. *Theoretical and Applied Mechanics, Vol.47*, 283-292.